Internet Electronic Journal of
Molecular Design

November 2003, Volume 2, Number 11, Pages 757–767

Editor: Ovidiu Ivanciuc

Special issue dedicated to Professor Nenad Trinajstić on the occasion of the 65th birthday
Part 5

Guest Editor: Douglas J. Klein

Hartree–Fock and Density Functional Studies on the Structure and Vibrational Frequencies of *N*–2–(6–Aminopyridine)–*N′*–arylthioureas

Shridhar P. Gejji and Kaustubh A. Joshi

Department of Chemistry, University of Pune, Pune 411 007, India

Received: August 30, 2003; Revised: October 7, 2003; Accepted: October 12, 2003; Published: November 30, 2003

Citation of the article:

S. P. Gejji and K. A. Joshi, Hartree–Fock and Density Functional Studies on the Structure and Vibrational Frequencies of *N*–2–(6–Aminopyridine)–*N′*–arylthioureas, *Internet Electron. J. Mol. Des.* **2003**, *2*, 757–767, http://www.biochempress.com.

Inter*net* Electronic Journal of Molecular Design

BioChem Press
http://www.biochempress.com

Hartree–Fock and Density Functional Studies on the Structure and Vibrational Frequencies of *N*–2–(6–Aminopyridine)–*N′*–arylthioureas[#]

Shridhar P. Gejji* and Kaustubh A. Joshi

Department of Chemistry, University of Pune, Pune 411 007, India

Received: August 30, 2003; Revised: October 7, 2003; Accepted: October 12, 2003; Published: November 30, 2003

Internet Electron. J. Mol. Des. **2003**, *2* (11), 757–767

Abstract

Motivation. The structure, charge distribution in terms of molecular electrostatic potentials and frequencies of normal vibrations of biologically important molecular systems, namely *N*–2–(6–aminopyridine)–*N′*–2–methoxyphenylthiourea **1**, *N*–2–(6–aminopyridine)–*N′*–4–chlorophenylthiourea **2**, *N*–2–(6–aminopyridine)–*N′*–4–nitrophenylthiourea **3** have been derived. These structural and vibrational characteristics provide insights for understanding of molecular interactions.

Method. Hartree–Fock and hybrid density functional methods employing Becke's three–parameter exchange with Lee, Yang, Parr correlation functional and with the Perdew Wang functional as well, have been carried out. Electrostatic potential and its topography have been analyzed in terms of critical points.

Results. Theoretically predicted structural parameters of these molecules compare well with those determined from the X–ray diffraction experiments. The Hartree–Fock calculations predict nonplanar structure around the C–N bond of the substituted phenylthiourea in **1**, **2** and **3**. Electrostatic potential reveals that the intermolecular hydrogen–bonded network in **3** extends *via* NO_2 group unlike S···H interactions present in **1** or **2**.The assignments of normal vibrations have shown that the N_3H_6 stretching of the thioamide has been influenced by substitution on the phenyl ring.

Conclusions. The present work reveals that hydrogen bonded network extends through the C=S···H interactions in **1** and **2** compared to **3** wherein this has been facilitated through the nitro group. The vibrations of thioamide group in these molecules are sensitive to the substituent on the phenyl ring.

Keywords. Hartree Fock; hybrid density functional; molecular electrostatic potential; hydrogen bonding.

1 INTRODUCTION

Synthesis and characterization of substituted *N*–2–pyridyl–*N′*–arylthioureas have been of considerable interest in the recent literature [1–12] due to the potential medical importance of substituted arylthioureas. The investigations of structure and charge distributions in these molecular systems possibly enable one to predict the structure–activity relationships. Recently the crystal

---

[#] Dedicated to Professor Nenad Trinajstić on the occasion of the 65th birthday.

* Correspondence author; phone: +91–020–5691728; fax: +91–020–5691728; E–mail: spgejji@chem.unipune.ernet.in.

structures of *N*–2–(6–aminopyridine)–*N′*–2–methoxyphenylthiourea (6AmTu2OMe) (**1**), *N*–2–(6–aminopyridine)–*N′*–4–chlorophenylthiourea (6AmTu4Cl) (**2**), *N*–2–(6–aminopyridine)–*N′*–4–nitrophenylthiourea (6AmTu4NO$_2$) (**3**) have been determined from the X–ray diffraction experiments [12]. These molecular systems are particularly interesting since it has been inferred that the presence of amino group on pyridine ring facilitates intermolecular hydrogen bonding *via* the N$_4$H hydrogen and the thione sulfur in addition to the intramolecular N–H–N interactions. Particularly, the *N*–phenyl analogs of *N*–2–pyridyl–*N′*–arylthioureas are known to be strong inhibitors of human enteroviruses. As a pursuit of this the structure, charge distributions of 6AmTu2OMe, 6AmTu24Cl, 6AmTu4NO$_2$ in terms of the topography of molecular electrostatic potential and the frequencies of normal vibrations have been derived by employing the quantum mechanical *ab initio* Hartree–Fock and hybrid density functional methods. The computational method has been outlined below.

2 COMPUTATIONAL METHOD

LCAO–MO–SCF restricted Hartree–Fock (HF) calculations have been carried out on the three substituted arylthioureas **1**, **2** and **3** with Gaussian 94 program [13] using the internally stored 6–31G (d,p) basis set. The stationary point geometries with respect to the nuclear coordinates were obtained by the simultaneous relaxation of all the geometric parameters using the analytical gradient method [14]. The geometries thus derived were subjected to optimizations using hybrid density functional methods incorporating, the Becke's three–parameter exchange with correlation functionals given by Lee, Yang and Parr (B3LYP) [15,16] and by Perdew and Wang (B3PW91) [17–19]. The molecular electrostatic potential (MESP) $V(\mathbf{r})$ at a point $\mathbf{r}$ due to a molecular system with nuclear charges $\{Z_A\}$ located at $\{R_A\}$ and the electron density $\rho(\mathbf{r})$ has been defined as:

$$V(\mathbf{r}) = \sum_{A=1}^{N} \frac{Z_A}{|\mathbf{r} - \mathbf{R}_A|} - \int \frac{\rho(\mathbf{r}')\mathrm{d}^3\mathbf{r}'}{|\mathbf{r} - \mathbf{r}'|} \qquad (1)$$

In above equation N is the total number of nuclei in the molecule and the two terms refer to the bare nuclear potential and the electronic contributions, respectively. Balancing of these two terms brings about effective localization of electron–rich regions in the molecular system. The MESP topography is mapped by examining the eigenvalues of the hessian matrix at the point where the gradient $V(\mathbf{r})$ vanishes. The MESP critical points (CPs) were located using a fortran code Univis–2000 [20,21]. The Fortran program Univis–2000 [20,21] was used for visualization of the MESP topography. These MESP CPs can be characterized [22,23] in terms of an ordered pair (rank, signature), which can further be grouped into three sets, *viz*., (3, +3), (3, +1) and (3, –1). The (3, +3) set corresponds to the set of minima and the remaining ones to the saddle points. Harmonic vibrational frequencies were obtained from the diagonalization of force constant matrix. Normal vibrations were assigned by visualizing the displacement of atoms around their equilibrium positions by using a program code Univis–2000 [20,21].

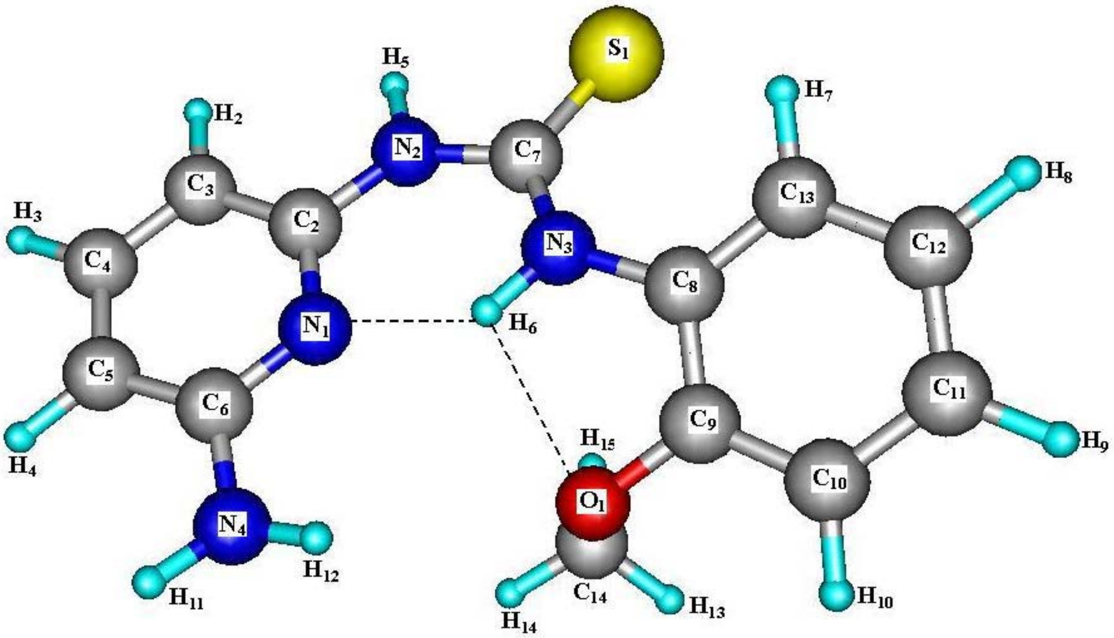

Figure 1a. *N*–2–(6–aminopyridine)–*N′*–2–methoxyphenylthiourea **1**.

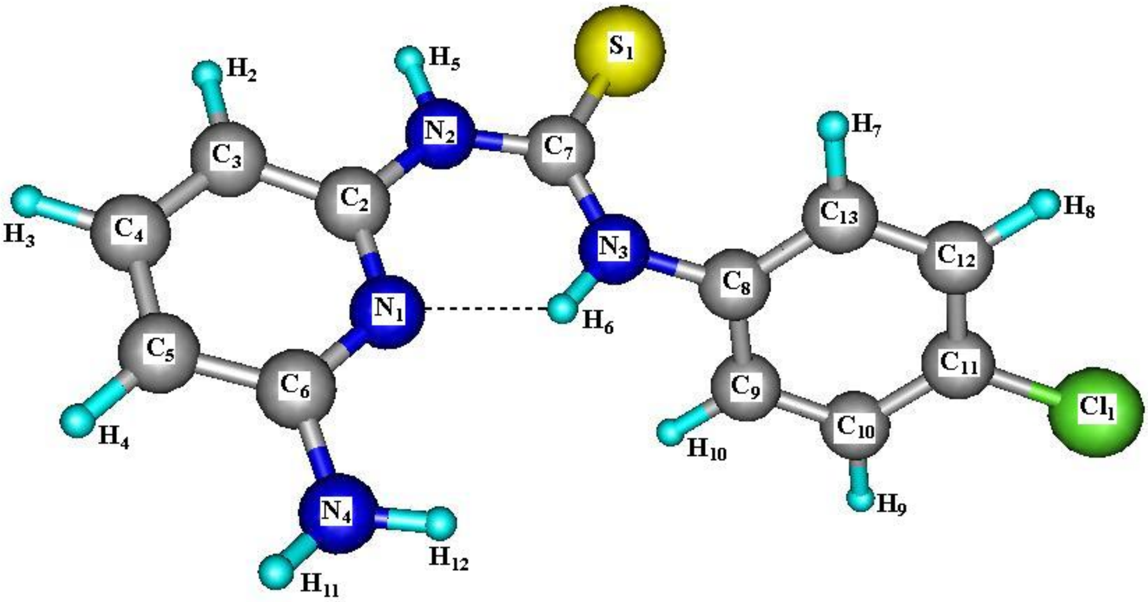

Figure 1b. *N*–2–(6–aminopyridine)–*N′*–4chlorophenylthiourea **2**.

3 RESULTS AND DISCUSSION

Optimized geometries of **1**, **2** and **3** alongwith the atomic labels used have been displayed in Figures 1a–1c. Selected bond– distances and angles of **1** from the Hartree–Fock and the hybrid density functional optimizations are compared with the corresponding ones determined from the X–

ray diffraction experiment in Table1. As may readily be noticed the HF/6–31G(d,p) predicted bond lengths, except for N_1C_2 and N_1C_6 distances, agree within 0.007 Å compared to the corresponding experimental values.

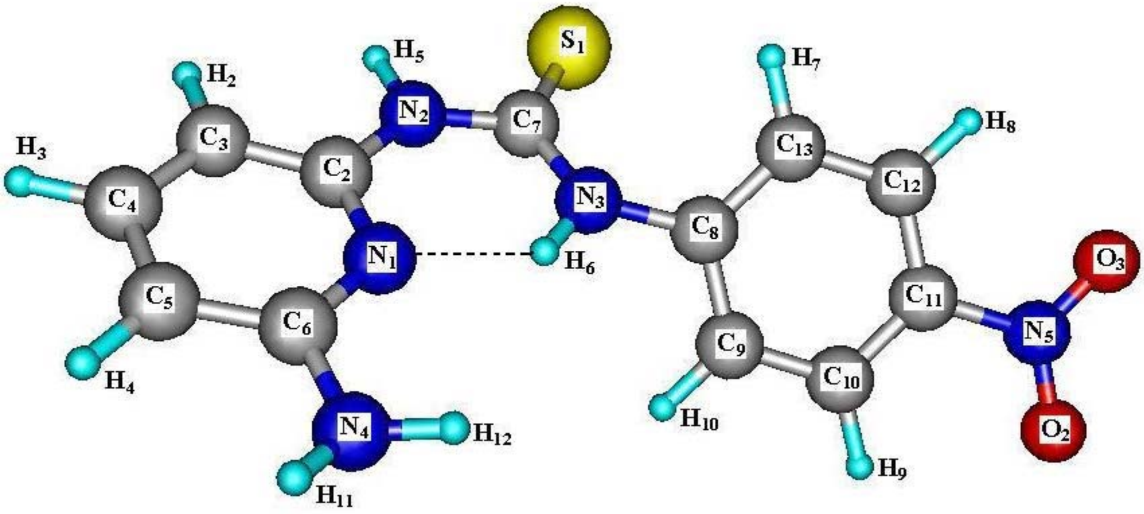

Figure 1c. N–2–(6–aminopyridine)–N’–4–nitrophenylthiourea **(3)**

These calculations predict the presence of bifurcated hydrogen bonds from the thioamide proton, viz., N_1–H_6 (1.881 Å) and H_6–O_1 (2.225 Å), leading to six– and five–membered rings, respectively, with the latter being 27° below the plane of the pyridine. Thus the predicted O_1–H_6 bond distance is 0.055 Å shorter than the corresponding bond distances from the X–ray data. Bond angles obtained from the HF and hybrid density functional methods agree within 2°. A closure of $S_1C_7N_3$ and $C_7N_3C_8$ bond angles ranging from 4° to 7° in a crystal was observed relative to those predicted for the gas phase.

The rest of the bond angles generally are in good agreement with the X–ray data. The (6–amino–pyridin–2–yl)thiourea and the anisole groups in **1** from the B3LYP and B3PW91 calculations are predicted to be nearly planar. On the other hand anisole and the (6–amino–pyridin–2–yl)thiourea groups in **1** orient mutually with an angle of 32° in the HF optimised structure relatively in better agreement with the experimental data. It should be remarked here that the optimized structure of **1** in a gas phase is quite different than that in the crystal when the orientation of the methyl group with respect to the phenyl ring has been taken into account. In the free molecule the rotation of the methyl group by 89^{o} about the CO bond (cf. Figure 1a) lowers the energy by 4.3 kJ mol^{-1} compared to the stationary geometry (confirmed to be the local minimum by vibrational frequencies) derived by using ORTEP diagram of the experiment [12].

Table 1. Optimized geometrical parameters (bond lengths in Å and bond angles in °) for **1**

	HF	B3PW91	B3LYP	Expt.
r(S_1C_7)	1.686	1.678	1.685	1.683(3)
r(N_1C_2)	1.318	1.335	1.337	1.329(3)
r(N_1C_6)	1.327	1.340	1.343	1.353(3)
r(N_2C_2)	1.390	1.389	1.394	1.397(3)
r(N_2C_7)	1.372	1.392	1.396	1.366(3)
r(N_3C_7)	1.328	1.348	1.352	1.328(3)
r(N_3C_8)	1.412	1.399	1.405	1.426(3)
r(C_9O_1)	1.368	1.384	1.390	1.375(3)
r(C_6N_4)	1.364	1.370	1.377	1.363(4)
r($H_6\cdots N_1$)	1.882	1.757	1.780	1.98(3)
r($H_6\cdots O_1$)	2.253	2.205	2.206	2.800
a($C_2N_1C_6$)	119.8	119.9	119.9	117.4(3)
a($N_1C_2C_3$)	123.0	122.6	122.6	124.1(3)
a($N_1C_2N_2$)	118.7	117.8	117.9	118.0(3)
a($N_2C_2C_3$)	118.4	122.6	119.6	117.9(3)
a($C_2N_2C_7$)	132.8	132.0	132.2	131.5(3)
a($S_1C_7N_2$)	116.4	116.8	116.8	118.1(2)
a($N_2C_7N_3$)	116.1	114.5	114.6	118.1(2)
a($S_1C_7N_3$)	127.5	128.7	128.6	123.8(2)
a($C_7N_3C_8$)	131.2	132.0	132.2	125.0(2)
a($N_1C_6N_4$)	115.8	115.3	115.3	115.8(3)
d($C_7N_3C_8C_{13}$)	32.4	13.9	13.7	69.2(0.09)
d($N_1C_2N_2C_7$)	3.4	3.9	3.6	4.92(0.09)

Table 2. Optimized geometrical parameters (bond lengths in Å and bond angles in °) for **2**

	HF	B3PW91	B3LYP	Expt.	Expt.
r(S_1C_7)	1.683	1.676	1.683	1.683(3)	1.680(3)
r(N_1C_2)	1.321	1.339	1.342	1.331(3)	1.329(3)
r(N_1C_6)	1.328	1.343	1.345	1.344(3)	1.350(3)
r(N_2C_2)	1.390	1.389	1.394	1.397(4)	1.411(3)
r(N_2C_7)	1.370	1.389	1.393	1.359(3)	1.353(3)
r(N_3C_7)	1.329	1.350	1.353	1.329(3)	1.343(3)
r(N_3C_8)	1.421	1.403	1.409	1.415(3)	1.420(3)
r($C_{11}Cl_1$)	1.744	1.747	1.760	1.737(3)	1.746(3)
r(C_6N_4)	1.366	1.372	1.377	1.374(4)	1.365(4)
r($H_6\cdots N_1$)	1.936	1.802	1.827	1.980(2)	2.000(3)
a($C_2N_1C_6$)	119.2	119.0	119.0	117.5(3)	116.9(2)
a($N_1C_2C_3$)	123.1	122.9	122.8	123.3(3)	124.5(3)
a($N_1C_2N_2$)	119.3	118.7	118.8	118.2(3)	117.3(3)
a($N_2C_2C_3$)	117.6	118.4	118.3	118.5(3)	118.2(3)
a($C_2N_2C_7$)	133.2	133.0	133.1	131.8(3)	132.3(3)
a($S_1C_7N_2$)	117.5	117.0	116.9	119.8(2)	119.4(2)
a($N_2C_7N_3$)	116.8	114.5	114.6	116.7(3)	115.9(3)
a($S_1C_7N_3$)	125.7	128.6	128.6	123.5(3)	124.7(2)
a($C_7N_3C_8$)	126.8	131.0	131.7	127.4(3)	126.5(3)
a($N_1C_6N_4$)	116.2	116.0	116.0	116.4(3)	115.7(3)
d($C_7N_3C_8C_{13}$)	63.7	21.8	20.1	67.94(0.10)	48.2(0.09)
d($N_1C_2N_2C_7$)	2.4	3.7	3.6	4.66(0.15)	12.25(0.15)

The geometrical parameters of **2** from the HF and the density functional methods have been reported with those obtained from the X–ray diffraction data in Table 2. Thus it may be inferred that the ortho– or para– substitution on the phenyl ring influence the relative orientation of the phenyl and the (6–amino–pyridin–2–yl)thiourea groups. Bond– distances and angles, however, are predicted to be relatively insensitive to such a substitution. Further the angle between the planes $C_7N_3C_8$ and $N_3C_8C_{13}$ from the HF theory (nearly 64°) agrees well with 68° found in one of the observed data sets.The experiment data sets in reference 12 show only marginal differences for bond– distances and angles.

In Table 3 the optimized bond– lengths and angle parameters of **3** from different theoretical methods and those obtained from the X–ray diffraction experiments are shown.

Table 3. Optimized geometrical parameters (bond lengths in Å and bond angles in °) for **3**

	HF	B3PW91	B3LYP	Expt.
r(S_1C_7)	1.679	1.673	1.680	1.679(4)
r(N_1C_2)	1.321	1.339	1.342	1.334(4)
r(N_1C_6)	1.329	1.343	1.346	1.343(4)
r(N_2C_2)	1.392	1.391	1.396	1.407(4)
r(N_2C_7)	1.366	1.386	1.390	1.363(4)
r(N_3C_7)	1.335	1.356	1.360	1.346(4)
r(N_3C_8)	1.412	1.394	1.400	1.402(4)
r($C_{11}N_5$)	1.456	1.458	1.463	1.453(4)
r(C_6N_4)	1.365	1.370	1.376	1.357(5)
r($H_6 \cdots N_1$)	1.912	1.791	1.816	1.91(4)
a($C_2N_1C_6$)	119.2	119.0	118.9	118.2(3)
a($N_1C_1C_3$)	123.2	123.0	123.0	123.3(3)
a($N_1C_1C_2$)	119.2	118.7	118.8	118.1(3)
a($N_2C_2C_3$)	117.6	118.3	114.3	118.6(3)
a($C_2N_2C_7$)	133.3	133.1	133.3	132.0(3)
a($S_1C_7N_2$)	117.5	117.1	117.1	118.4(2)
a($N_2C_7N_3$)	116.2	114.1	114.3	115.0(3)
a($S_1C_7N_3$)	126.3	128.7	128.7	126.6(3)
a($C_7N_3C_8$)	128.6	131.9	132.2	132.7(3)
a($N_1C_6N_4$)	116.2	116.2	116.2	116.2(3)
d($C_7N_3C_8C_{13}$)	49.4	12.3	11.1	7.42(0.13)
d($N_1C_2N_2C_7$)	2.3	4.2	4.0	3.18(0.11)

Unlike for **1** and **2** the B3LYP predicted geometrical parameters of **3** are in better agreement with the corresponding experimental data. The N_2C_7 and C_6N_4 bond distances within the B3LYP framework, however, turn out to be respectively, 0.027 Å and 0.018 Å, longer than their experimental counterparts. As observed in the X–ray diffraction data [12] the N_3C_8 bond distance in this case shows a marginal decrease compared to the corresponding distance in **1**. The predicted structures in gas phase, however, do not support these conclusions. Further the $C_7N_3C_8C_{13}$ dihedral angle (11°) from the B3LYP calculations compares favorably with the experiment [12].

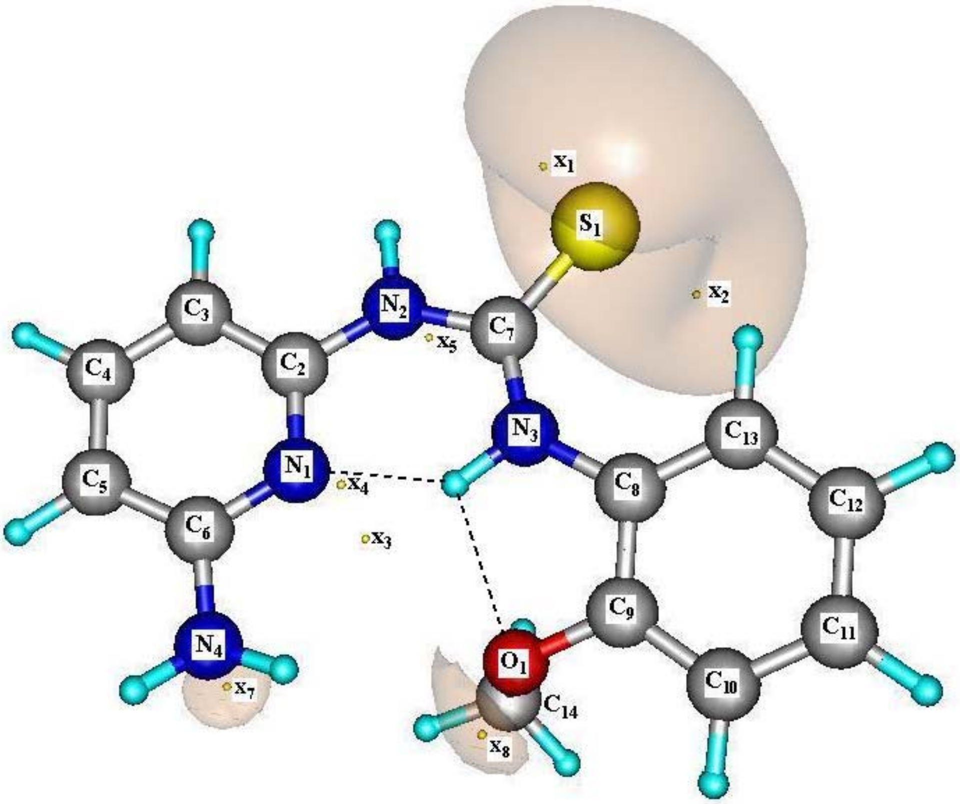

Figure 2a. MESP isosurface ($V = -107.65$ kJ mol^{-1}) and (3, +3) minima for **1**.

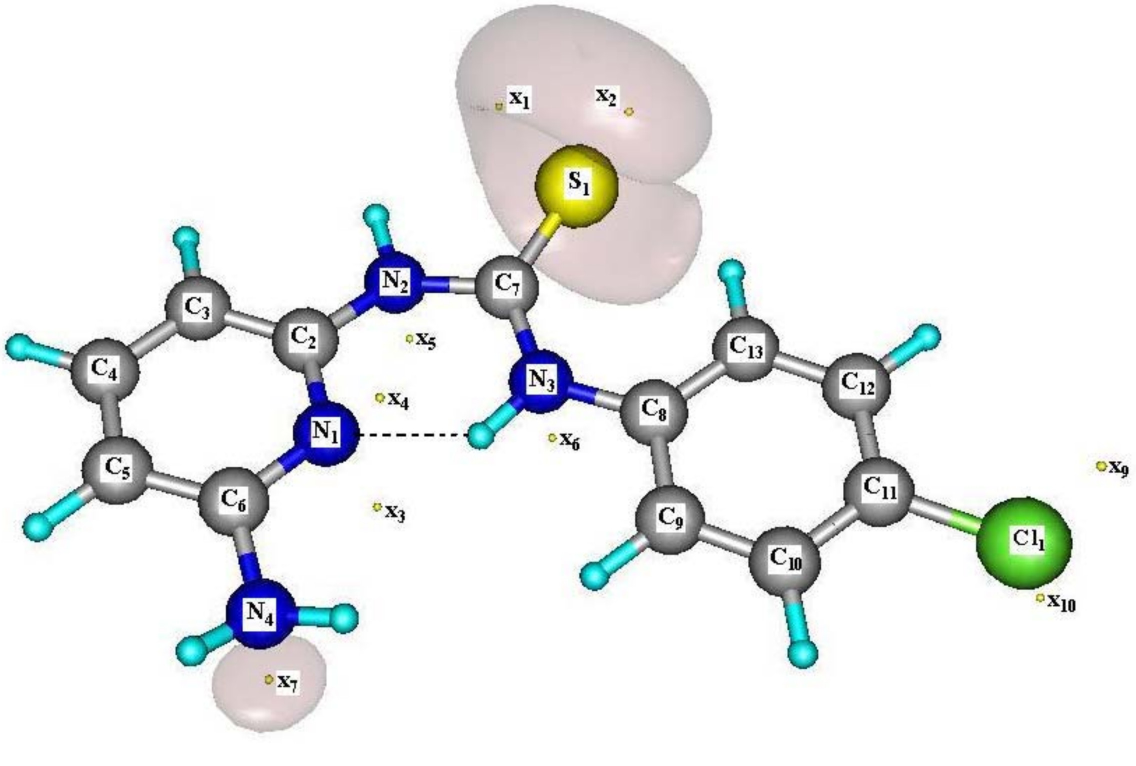

Figure 2b. MESP isosurface ($V = -107.65$ kJ mol^{-1}) and (3, +3) minima for **2**.

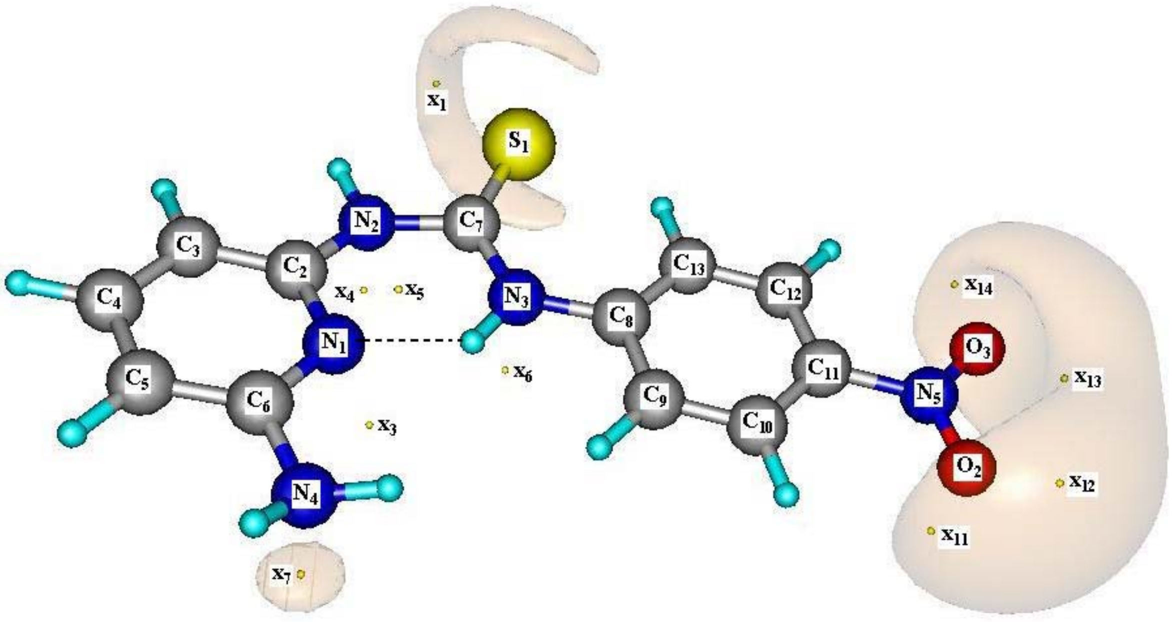

Figure 2c. MESP isosurface ($V = -107.65$ kJ mol^{-1}) and (3, +3) minima for **3**.

As pointed out in the preceding section the MESP brings about the effective electron localization. The MESP isosurfaces with $V = -107.65$ kJ mol^{-1} of **1**, **2** and **3** are depicted in Figure 2a–2c along with the critical points representing the MESP minima, denoted by $\mathbf{x_1}$, $\mathbf{x_2}$,…. Thus electron–rich regions near sulfur in **1** are observed to be large compared to those in **2** or **3** as a result of both the inductive and mesomeric effects from the amino group at ortho position of pyridine, which engender the $S\cdots H$ hydrogen bonded network in a crystal. The conclusions drawn for **2** are qualitatively similar. This has also been supported by the MESP value at the critical point (minimum) near sulfur shown in Table 4. It may be inferred that the intermolecular hydrogen bonding in **3**, however, facilitates through the NO_2 group.

Table 4. The MESP minima (in kJmol^{-1}) for *N*–2–(6–aminopyridine)–*N*′–arylthioureas

		1	2	3
S_1	x_1	−200.5	−141.7	−129.8
	x_2	−191.4	−156.4	
N_1	x_3	−86.2	−47.1	−41.5
	x_4	−71.2	−65.6	−23.9
N_2	x_5	−38.4	−73.1	−36.4
N_3	x_6		−56.1	−19.2
N_4	x_7	−152.5	−173.6	−155.2
O_1	x_8	−144.3		
C_1	x_9		−76.5	
	x_{10}		−75.2	
O_2	x_{11}			−228.4
	x_{12}			−150.3
O_3	x_{13}			−228.8
	x_{14}			−159.1

The vibrational frequencies of **1**, **2** and **3** are compared with those of the phenyl–thiourea and the 2–aminopyridine in the following. The B3LYP/6–31G(d,p) calculated harmonic vibrational frequencies are reported in Table 5. A comparison of phenylthiourea and **1** predicts that both the 3702 cm^{-1} and 3559 cm^{-1} free NH_2 vibrations of phenylthiourea disappear on combining with the 2–aminopyridine and peak at ~3625 cm^{-1} has been predicted instead. It may be remarked here that the intense N_3H_6 stretching in *N*–2–(6–aminopyridine)–*N'*–arylthioureas is sensitive to the substituent on phenyl ring. For **1** this vibration occurs at 3203 cm^{-1} compared to that in **2** and **3** which has been upshifted by ~ 80 cm^{-1} and 48 cm^{-1}, respectively. A downshift of the N_3H_6 stretching in **1**, **2** and **3** relative to phenyl–thiourea, results from the N_3—H_6 and pyridyl nitrogen interactions.

Table 5. Selected B3LYP vibrational frequencies (cm^{-1}) of 2–aminopyridine, phenylthiourea, **1**,**2** and **3**

Assignment	2–aminopyridine	Phenylthiourea	1	2	3
N_4H stretch	3705(22)		3702(55)	3717(31)	3720(34)
	3583(31)		3562(68)	3597(38)	3600(41)
N_2H stretch		3702(47)	3628(53)	3625(54)	3622(55)
		3559(44)			
N_3H stretch		3575(71)	3203(617)	3283(592)	3251(677)
C_7N_3H rock		1598(404)	1677(578)	1688(505)	1696(439)
HN_4H scissor	1638(25)		1643(182)	1644(7)	1645(20)
N_1C_6 stretch + C_3C_4 stretch	1627(29)		1642(200)	1641(391)	1637(624)
C_2N_2H rock			1555(137)	1559(515)	1559(482)
$C_9C_{10}H$, $C_{12}C_{13}H$ rock		1537(33)	1529(137)	1535(214)	1538(112)
C_2C_3H rock	1528(62)		1512(104)	1513(57)	1510(83)
	1488(76)		1498(97)	1498(246)	1499(205)
C_7N_3 stretch		1438(424)	1402(360)	1408(521)	1405(41)
C_3C_4H, C_6C_5H, $C_9C_{10}H$, $C_{12}C_{11}H$			1171(230)	1178(295)	1181(260)
rock	1150(1)	1150(52)			
C_7S_1 stretch		737(29)	764(14)	781(31)	773(29)

Some intense vibrations for **1**, **2** and **3** emerge in the region 1400 cm^{-1} – 1700 cm^{-1}. The 1598 cm^{-1} and 1438 cm^{-1} normal vibrations in thiourea assigned to $C_7N_3H_6$ rocking and C_7N_3 stretching, respectively, are of interest. The former vibration has been upshifted by 79 cm^{-1} – 98 cm^{-1} whereas the latter downshifts to ~1405 cm^{-1} in **1**, **2** and **3**. An intense vibration near 1560 cm^{-1} assigned to $C_2N_2H_5$ rocking, has been predicted for **1**, **2** and **3** as well.

The intense vibrations due to pyridine ring are predicted to occur near ~1640 cm^{-1}. For **1**, **2** and **3**, the 1170 – 1180 cm^{-1} region presents intense vibrations, which are strongly coupled and difficult to correlate with those in phenylthiourea or aminopyridine. The C=S stretching (737 cm^{-1}) of phenylthiourea is sensitive to the substituent on the phenyl ring and upshift to 764 cm^{-1} – 781 cm^{-1} has been predicted for **1**, **2** and **3**.

4 CONCLUSIONS

The present calculations predict that the N_1–H_6 and the H_6–O_1 bifurcated hydrogen bonded interactions of thioamide group lead to six– and five–membered rings in the ortho–substituted derivative (**1**). HF predicted bond distances of thiourea group in **1**, **2** and **3** generally agree within 0.01 Å compared to those observed in experiment. In *o*–methoxy derivative the phenyl group and 2–aminopyridine orient mutually with an angle of 32°. For the para substituted chloro derivative the chlorophenyl ring has been pushed further below by 32° relative to 2–aminopyridine as compared to that in **1**. MESP topographical features reveal how the intermolecular hydrogen bonded network facilitates possibly through the NO_2 group in **3** and *via* the C=S···H interactions for **1** and **2**. The vibrations of thioamide group in these molecules are sensitive to the substitution on the phenyl ring, partly attributed to the inductive and mesomeric effects. A downshift of ~300 cm^{-1} for the N_3–H stretching in these molecules compared to the corresponding vibration in free phenylthiourea has been predicted as a result of the intramolecular hydrogen bonded interactions.

Acknowledgment

SPG is grateful to the Council of Scientific and Industrial Research (CSIR Project 01(1772)/02/EMR–II), New Delhi, India. KAJ thanks CSIR for the Junior research fellowship.

5 REFERENCES

[1] D. X. West, A. K. Hermetet, L. J. Ackerman, J. Valdés–Martínez, S. Hernández–Ortega, 3–Phenyl–1–(2–pyridyl)thiourea, *Acta. Crystallogr.* C55 **1999**, 811.

[2] J. Valdés–Martínez, S. Hernández–Ortega, D. X. West, L. J. Ackerman, J. K. Swearingen, A. K. Hermetet, Structural and spectral studies on *N*–(2–pyridyl)–*N′*–tolylthioureas, *J. Mol. Struct.* **1999**, *478*, 219.

[3] E. A. Sudbeck, J. D. Jennissen, T. K. Venkatachalam, F. M. Uckun, Inhibitor of HIV–1 reverse transcriptase: *N*–(5–bromo–2–pyridyl)–*N*–[2–(2,5–di–methoxyphenyl)ethyl]thiourea, *Acta Crystallogr.*, C55 **1999**, 2122.

[4] D. X. West, J. K. Swearingen, A. K. Hermetet, L. J. Ackerman, C. Presto, Structural and spectral studies on N–2–(4,6–lutidyl)–N’–tolylthioureas, *J. Mol. Struct.* **2000**, *522*, 27.

[5] D. X. West, J. K. Swearingen, A. K. Hermetet, L. J. Ackerman, Structural and spectral studies of *N*–2–(pyridyl)–, *N*–2–(4–,5–, and 6–picolyl)– and *N*–2–(4,6–lutidyl)–*N′*–2–methoxyphenylthioureas, *J. Mol. Struct.* **2001**, *562*, 95.

[6] W. Kaminsky, K. I. Goldberg, D. X. West, Synthesis and structures of two N,N’–bis(2–pyridinyl) thioureas and *N*–(2–pyridinyl)–*N′*(benzoyl)thiourea, *J. Mol. Struct.* **2002**, *605*, 9.

[7] L. F. Szczepura, K. K. Eilts, A.K. Hermetet, J. K. Swearingen, D. X. West, Structural and spectral studies of *N*–(2–pyridyl)–*N′*–(4–substitutedphenyl)thioureas, *J. Mol. Struct.* **2002**, *607*, 101.

[8] A. K. Hermetet, L.J. Ackerman, K. K. Eilts, T. K. Johnson, J. K. Swearingen, J. M. Giesen, K. I. Goldberg, W. Kaminsky, D. X. West, Structural, spectral and thermal studies of *N*–2–(4,6–lutidyl)–*N′*–chlorophenylthioureas, *J. Mol. Struct.* **2002**, *605*, 241.

[9] J. Valdés–Martínez, S. Hernández–Ortega, G. Espinosa–Perez, C. A. Presto, A.K. Hermetet, K.D. Haslow, L. J. Ackerman, L. F. Szczepura, K. I. Goldberg, J. M. Giesen, W. Kaminsky, D. X. West Structural, spectral and thermal studies of substituted *N*–(2–pyridyl)–*N′*–phenylthioureas, *J. Mol. Struct.* **2002**, *608*, 77.

[10] L. F. Szczepura, D. R. Kelman, A.K. Hermetet, L. J. Ackerman, K. I. Goldberg, K. A. Claborn, W. Kaminsky, D. X. West, Structural, spectral and thermal studies of *N*–2–(picolyl)–*N′*–4–chloro phenylthioureas, *J. Mol. Struct.* **2002**, *610*, 245.

[11] D. R. Kelman, L. F. Szczepura, K. I. Goldberg, W. Kaminsky, A. K. Hermetet, L.J. Ackerman, J. K. Swearingen, D. X. West, Structural, spectral and thermal studies of *N*–2–(4–picolyl)– and *N*–2–(6–picolyl)–*N′*–(2–bromophenyl)thiourea, *J. Mol. Struct.* **2002**, *610*, 143.

[12] D. R. Kelman, K .A. Claborn, W. Kaminsky, K. I. Goldberg, D. T. Li, D. X. West, Structural studies of *N*–2–(6–aminopyridine)–*N′*–arylthioureas, *J. Mol. Struct.* **2003**, *654*, 145.

[13] M. J. Frisch, G.W. Trucks, H. B. Schlegl, P. M. W. Gill, B. G. Johnson, M. A. Robb, J. R. Cheeseman, T. Keith, G. A. Petersson,J. A. Montgomery, K. Raghavachari, M. A. Al–Laham, V. G. Zakrzewski,J. V. Ortiz, J. B. Foresman, J. Ciosloski, B. B. Stefanov, A. Nanayakkara, M. Challacombe, C. Y. Peng, P.Y. Ayala, W. Chen, M. W. Wong, J. L. Andres, E.S. Replogle, R. Gomperts, R. L. Martin, D. J. Fox, J. S. Binkley, D. J. Defrees, J. Baker, J. P. Stewart, M. HeadGordon, C. Gonzalez, J. A. Pople, Gaussian 94 **1995**. Gaussian Inc., Pittsburgh PA.

[14] P. Pulay, Ab initio calculation of force constants and equilibrium geometries in polyatomic molecules. I. Theory, *Mol. Phys*. **1969**, *17*, 197.

[15] A. D. Becke, Density functional thermochemistry. III. The role of exact exchange, *J. Chem. Phys*. **1993**, *98*, 5684.

[16] C. Lee, W. Yang, R. G. Parr, Development of the Colle–Salvetti correlation–energy fromula into a functional of the electron density, *Phys. Rev. B* **1988**, *37*, 785.

[17] J. P. Perdew, J. A. Chevary, S. H. Vosko, K. A. Jackson, M. R. Pederson, D. J. Singh and C. Fiolhais, Atoms, molecules, solids and surface: applications of the generalized gradient approximation for exchange and correlation, *Phys. Rev. B* **1992**, 46.

[18] J. P. Perdew, J. A. Chevary, S. H. Vosko, K. A. Jackson, M. R. Pederson, D. J. Singh and C. Fiolhais, Atoms, molecules, solids and surface: applications of the generalized gradient approximation for exchange and correlation, *Phys. Rev. B* **1993**, 48.

[19] J. P. Perdew, K. Burke and Y. Wang, Generalized gradient approximation for the exchange–correlation hole of a many electron system *Phys. Rev. B* **1996**, *54*, 16533.

[20] A. C. Limaye, S. R. Gadre, Univis–2000: An indigenously developed comprehensive visualization package, *Curr. Sci.* (India) **2001**, *80*, 1298.

[21] S. R. Gadre, R. N. Shirsat, Electrostatics of Atoms and Molecules. Universities Press, Hyderabad (India) 2000.

[22] S. R. Gadre, I. H. Shrivastava, Shapes and sizes of molecular anions via topographical analysis of electrostatic potential, *J. Chem. Phys.* **1991**, *94*, 4384.

[23] S. R. Gadre, S. A. Kulkarni, I. H. Shrivastava, Molecular electrostatic potentials: A topographical study, *J. Chem. Phys*. **1992**, *96*, 5253.